Magnetic Damping of g-Jitter Driven Flows: 3-D Calculations

D. Y. Shang[A], B. Q. Li[A] and H. C. de Groh[B]

A 3-D numerical model is developed to represent the oscillating ~~thermal~~ natural convection induced in a cylindrical cavity filled with Ga-doped germanium ~~melt~~ with and without the presence of an external magnetic field. The model is developed based on the penalty-finite element solution of the equations describing the transport of momentum, heat and solutal element as well as the electromagnetic field distribution in the melt pool. Automatic time step control is applied to help speed up the calculations. Numerical simulations are conducted to study the convection and magnetic damping effects as a function of frequency, directions and amplitudes of g-jitter and also the direction and magnitudes of the applied magnetic fields. The results show that the g-jitter driven flow is time dependent and exhibits a complex recirculating convection pattern in three dimensions and that an applied magnetic field can be employed to suppress this deleterious convective flow and both magnitude and orientation of the applied field are important in magnetic damping of the g-jitter induced convective flows.

1. Introduction

Microgravity and magnetic damping are two mechanisms applied during the melt growth of semiconductor or metal single crystals to suppress buoyancy driven flows so as to improve macro and micro homogeneity of the crystals. As natural convection arises from gravity effects, microgravity offers a plausible solution to reduce the convective flow to achieve a desirable growth condition. However, flight experiments indicated that residual accelerations during space processing, or g-jitter, can cause considerable convection in the liquid pool, making it difficult to realize a diffusion controlled growth, as originally designed, when experiments were conducted in microgravity [1,2].

G-jitter is a phenomenon associated with microgravity environment and can have both steady state and transient effects on convective flows[4,5]. Measurements by accelerameters aboard space vehicles reveal that g-jitter is inherent with space environment and that it is three dimensional and random in nature and has a wide band of frequency[6]. Recently, the effect of g-jitter on fluid flow behavior in microgravity has been a subject of intensive research. Substantial work has been published to investigate convection flows in single crystal growth systems that are induced by both steady state and transient gravity perturbations under microgravity conditions. Numerical modeling results showed that the frequency, amplitude and spatial orientation of g-jitter are all important in affecting the convective flows[7-14]. The analyses further indicated that the most detrimental effect of g-jitter comes from the low frequency component with a large amplitude, especially when it is aligned perpendicularly with temperature gradient, which often is along the crystal growth direction. For crystal growth applications, the effects of the high frequency g-jitter components may be neglected.

Magnetic damping effects on the motion of an electrically conducting fluid originate from the interaction of the flow field with an externally applied magnetic field. This interaction induces an opposing Lorentz force that results in a reduction of melt flow velocities. The use of magnetic damping has been widely exploited in the materials industries to obtain more homogeneous semiconductors and metal crystals under terrestrial conditions. While magnetic damping on turbulent and thermal fluctuations on earth has been well established[15,16]; relatively little is known about the magnetic damping effect on the flow field generated by low frequency g-jitter in microgravity.

Because magnetic damping stems from a different origin than gravity, it may be superimposed over microgravity to further suppress the deleterious effects associated with g-jitter. This idea has been explored recently[15-17]. Both analytical and 2-D numerical analyses have been performed. The analytical solutions were derived for a configuration of a parallel plate thermal channel subject to both the oscillating gravity force and a transverse magnetic field and were used to serve a dual purpose of obtaining an asymptotic behavior of the system and of providing a check for numerical development. Numerical analyses were also conducted for a 2-D Bridgman-Stockbarger system for the growth of Gadoped germanium single crystals. These analyses showed that magnetic damping can be applied to reduce the g-jitter induced convective flows and the reduction of the velocity depends on the g-jitter frequency and applied magnetic field strength and direction.

A. School of Mechanical and Materials Engineering, Washington State University, Pullman, WA 99164, USA.
B. NASA Lewis Research Center, Cleveland, OH 44135, USA.

This paper describes a numerical investigation of magnetic damping on g-jitter induced fluid flow and mass transfer in a 3-D Brigdman-Stockbarger system for Ga-doped germanium single crystal growth under g-jitter conditions. For this purpose, a transient 3-D numerical model is developed based on the Galerkin finite element solution of magnetohydrodynamic equations governing the fluid flow behavior in the presence of time dependent gravity perturbations and an applied magnetic field. It is important to realize that g-jitter is inherently three dimensional and time dependent and thus a 3-D dimensional model is more appropriate to fully resolve the g-jitter driven flows with and without the present of a magnetic field.

2. Problem Statement

The problem to be considered is schematically represented in Figure 1 below. In essence, we consider a simplified 3-D model for the Bridgmann-Stockbroker growth of Ge-doped silicon single crystals where the phase change due to solidification is neglected and as such the top and bottom surfaces are assumed flat. The melt is fed from the above into the molten zone. Solidification takes place at the lower side and the single crystal is withdrawn from the below. For the Bridgman-Stockbarger system, the lower side marked by h_2 is insulated and the upper side wall is fixed at the same temperature as the top surface or melt inlet. In microgravity environment, g-jitter varies in time and orientation to induce convection in the molten zone. The magnetic field is imposed to damp the convective flows. Shown also in the figure is the cylindrical coordinate system used for the numerical analyses.

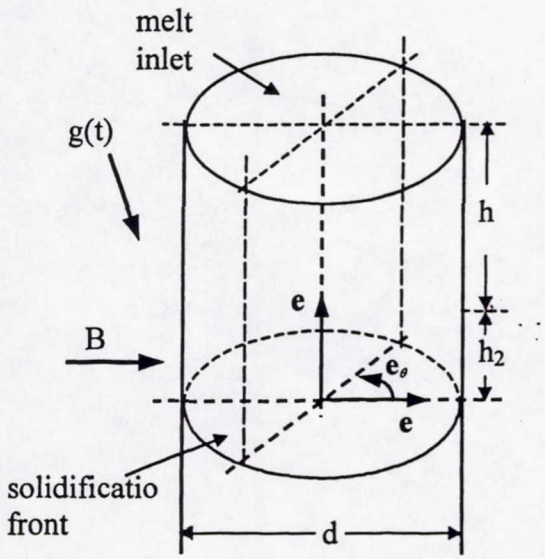

Fig. 1 Schematic representation of the 3-D model for magnetic damping studies.

The physical phenomena occurring in the system described above are governed by the Maxwell equations for the electromagnetic field distribution, the Navier-Stokes equations for fluid flow and the scalar transport equations for both heat and alloy element distributions. For systems like this, the magnetic Reynolds number is small. Also, we are primarily concerned with the flows generated by low frequency g-jitter components. As such, the induced magnetic field may be well neglected in comparison with the imposed magnetic field and the time variation of the induced electric field is also small. These considerations allow us to reduce the Maxwell equations to one equation for the electric potential[15-17]. With these taken into account, the mathematical equations governing the fluid flow, temperature and species distributions and electromagnetic phenomena in the melt system may be written in the nondimensional form as follows,

$$\nabla \cdot \mathbf{u} = 0 \tag{1}$$

$$\frac{\partial \mathbf{u}}{\partial t} + \mathbf{u} \cdot \nabla \mathbf{u} = -\nabla p + Pr\nabla^2 \mathbf{u} - RaPrTg^* + Ha^2 Pr(-\nabla\Phi + \mathbf{u} \times \mathbf{B}) \times \mathbf{B} \tag{2}$$

$$\frac{\partial T}{\partial t} + \mathbf{u} \cdot \nabla T = \nabla^2 T \tag{3}$$

$$\frac{Sc}{Pr}\left(\frac{\partial C}{\partial t} + \mathbf{u} \cdot \nabla C\right) = \nabla^2 C \tag{4}$$

$$\nabla^2 \Phi = \nabla \cdot (\mathbf{B} \times \mathbf{u}) = \mathbf{B} \cdot (\nabla \times \mathbf{u}) \tag{5}$$

The boundary conditions for the problem represent the physical constraints needed to solve the problem. For the present problem, the no slip conditions are applied at all the solid walls. Part of the side wall is thermally insulated and the other part is at a fixed temperature, the top and bottom walls are at the fixed temperatures and the electric current density is zero on the solid walls as no current can escape from the system, because the walls are electrically insulated as well. These conditions may be phrased in mathematical terms, viz.,

$$T = 0 \qquad \text{at } z = 0 \tag{6}$$

$$\mathbf{u} \cdot \mathbf{n} = \frac{Pe_g Pr}{Sc} \qquad \text{at } z = 0 \tag{7}$$

$$\mathbf{u} \times \mathbf{n} = 0 \qquad \text{at } z = 0 \tag{8}$$

$$\frac{\partial C}{\partial z} = Pe_g(1-k)C \quad \text{at } z=0 \qquad (9)$$

$$T = 1 \quad \text{at } z=1 \qquad (10)$$

$$\mathbf{u}\cdot\mathbf{n} = -\frac{Pe_g Pr}{Sc} \quad \text{at } z=1 \qquad (11)$$

$$\mathbf{u}\times\mathbf{n} = 0 \quad \text{at } z=1 \qquad (12)$$

$$\frac{\partial C}{\partial z} = Pe_g(C-1) \quad \text{at } z=1 \qquad (13)$$

$$\mathbf{u}\cdot\mathbf{n} = \frac{Pe_g Pr}{Sc} \quad \text{at } r=0.5 \qquad (14)$$

$$\mathbf{u}\times\mathbf{n} = 0 \quad \text{at } r=0.5 \qquad (15)$$

$$\mathbf{n}\cdot\nabla C = 0 \quad \text{at } r=0.5 \qquad (16)$$

$$T = 1 \quad \text{at } r=0.5,\ h_1/d < z < 1 \qquad (17)$$

$$\mathbf{n}\cdot\nabla T = 0 \quad \text{at } r=0.5,\ 0 < z < h_1/d \qquad (18)$$

$$\mathbf{n}\cdot\nabla\Phi = 0 \quad \text{at } z=0,\ 1,\ r=0.5 \qquad (19)$$

In the above equations, **u** is the velocity, p the pressure, T the temperature, $\mathbf{g}^*$ gravity vector, Φ the electric potential, **B** the applied magnetic field vector, t the time, C the concentration, n the outward normal, k the solutal partetion coeffecient between the solid and liquid phase, and **n** the outward normal. Also the following scales have been used in nondimensionalization, $L=d$, $U=\alpha/L^2$, $t_0=d^2/\alpha$, $P=\rho\alpha^2/d^2$ and $\Phi=\alpha B$, where ρ is the density, α the thermal diffusivity and B the applied magnetic field strength. The temperature is nondimensionalized as $T=(\theta-T_m)/(T_h-T_m)$ where θ is the dimensional temperature, T_h the melt inlet temperature and T_m the melting point. The nondimensionalization process also resulted in a set of nondimensional system parameters, which are given below,

Rayleigh number: $$Ra(t) = \frac{\beta g(t)(T_h - T_m)L^3}{\nu\alpha}$$

Prandtl number $$Pr = \frac{\nu}{\alpha}$$

Schmidt number $$Sc = \frac{\nu}{D}$$

Peclet number (species): $$Pe_g = \frac{V_m L}{D}$$

Hartman number $$Ha = BL\sqrt{\frac{\sigma_m}{\mu_m}}$$

with g being the earth gravity, β the thermal expansion, ν the kinematic viscosity, D the diffusion coefficient of the species, V_m the growth velocity, σ_m the electrical conductivity and μ_m the molecular viscosity.

3. The finite element solution

The above equations along with the boundary conditions are solved using the Galerkin finite element method. Applying the standard finite element procedures to the above equations and carrying out involved algebraic operations, one has the following set of matrix equations for the unknowns defined at the nodal points,

$$\mathbf{M}\dot{\mathbf{U}} + \mathbf{K(U)U} + \frac{1}{\varepsilon}\mathbf{C_P M}_p\mathbf{C_P}^T\mathbf{U} + \mathbf{C_B T} = \mathbf{F_U} \qquad (20)$$

$$\mathbf{M}_T\dot{\mathbf{T}} + \mathbf{K}_T\mathbf{(U)T} = \mathbf{F}_T \qquad (21)$$

$$\mathbf{M}_C\dot{\mathbf{C}} + \mathbf{K}_C\mathbf{(U)C} = \mathbf{F}_C \qquad (22)$$

$$\mathbf{K}_\Phi\Phi + \mathbf{C}_\Phi\mathbf{U} = \mathbf{F}_\Phi \qquad (23)$$

where now **U** is a global vector containing all the nodal values of u, v and w. **C**, **T** and Φ are global nodal concentration, temperature and electric potential vectors respectively. **M** is the mass matrix, $\mathbf{K(U)}\equiv\mathbf{N(U)}+\mathbf{K}_\mu$ is the stiffness matrix, where $\mathbf{K}_\mu$ is the diffusion stiffness matrix, and **N(U)** is the advection stiffness matrix. $\mathbf{C}_p$ is gradient matrix, $\mathbf{C_B}$ the buoyancy matrix and $\mathbf{F_U}$ the "force" vector which incorporates the Lorentz force term and the boundary conditions. In the temperature, penalty continuum and electric potential equations, the subscripts T, P and Φ refer to the corresponding sets of coefficients. The above matrix equations are solved using the successive substitution method and the time derivatives are approximated using the implicit finite difference scheme. Both variable time steps with automatic error tracking and time step automation and fixed time steps may be applied. The majority of the results presented in the report are calculated using the fixed time steps.

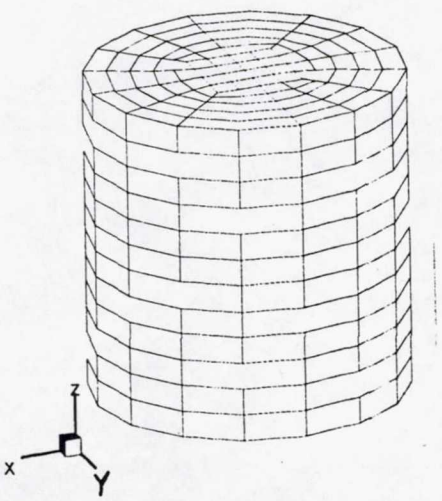

Fig.2 Finite element mesh used for numerical simulations.

4. Results and Discussion

The finite element model developed above enables the prediction of electromagnetic field, velocity, temperature and solutal distributions in the 3-D cavity under the influence of both g-jitter and an applied magnetic field. A selection of computed results is presented below. All the results were computed using 8-node brick elements and a typical mesh for the calculations is given in Figure 2. We are particularly interested in the effects of transient g-jitter and magnetic damping. Thus the results presented below represent the situation where a steady state thermal and fluid flow condition is established by a steady gravity force in microgravity and then g-jitter is introduced to perturb the fluid flow field. To investigate the magnetic damping effects, the magnetic field is switched on at the same time the g-jitter starts to act. As stated earlier, g-jitter is random and 3-dimesnional in nature. However, to obtain some fundamental insight into the g-jitter driven flow and magnetic damping effects, we consider a typical component of a synthesized g-jitter force and a simplified magnetic field arrangement. The physical properties for the simulations are given in an earlier publication[20].

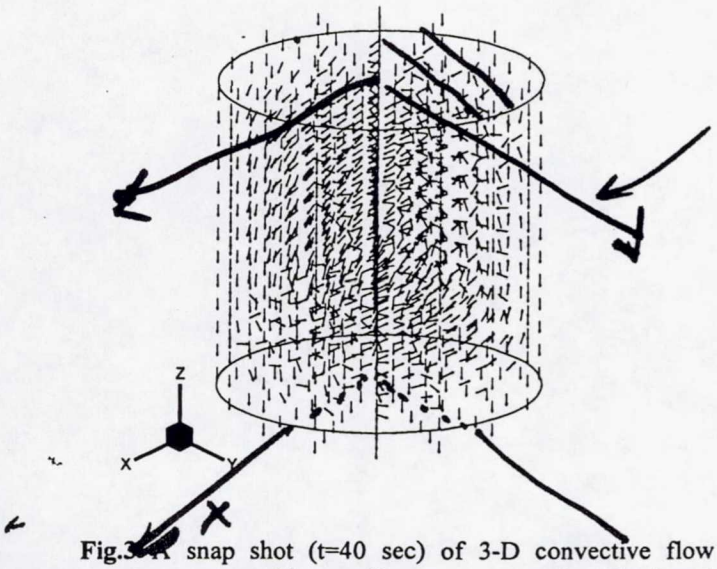

Fig.3 A snap shot (t=40 sec) of 3-D convective flow structure generated by a g-jitter component (amplitude = 1 x 10^{-3} g_0, g_0 the earth gravity constant and frequency = 0.1 Hz) oscillating in the x direction. The time is measured from the point at which the time varying g-jitter force starts to act on the fluid.

Convective flows in this system are bound to be complex because of the interaction of the incoming flows and the convection cells generated by g-jitter. Figure 3 plots such a typical fluid flow structure induced by a time varying g-jitter force 40 seconds after it becomes effective. The initial thermal and flow field is generated by a constant g-jitter force that has been discussed in detail by Pan *et al*[20]. In this case, g-jitter is assumed to act in the x-direction only but varying harmonically with time following a sine function. It is clearly seen from the figure that the convection pattern is complex and g-jitter force strongly perturbs otherwise a plug flow field from the top to bottom that would result only from the inlet inertia.

For the system under consideration, the *Pr* number is small, suggesting that the g-jitter driven flows have little effect on the temperature distribution. This has been confirmed in this 3-D numerical study and as in the two dimensional case studied earlier[20] the thermal transport in the system is by conduction only. This holds true also when an external magnetic field is imposed.

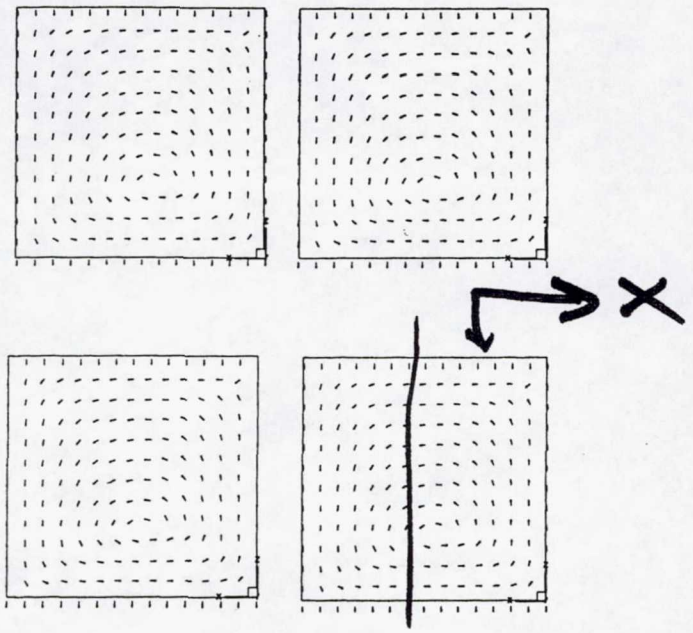

Fig. 4 Velocity field in the x-z plane at different time steps (viewed from the positive y-axis, same g-jitter as in Fig. 3): (a) t=5 sec, (b) t=10 sec, (c) t=35 sec, and (d)=40 sec.

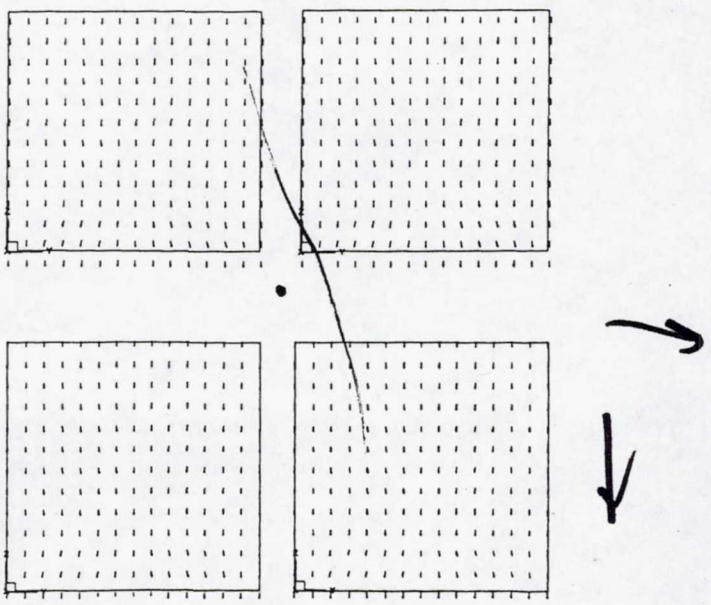

Fig. 5 Velocity field in the y-z plane at different time steps (viewed from the negative x-axis, same g-jitter as in Fig. 3): (a) t=5 sec, (b) t=10 sec, (c) t=35 sec, and (d)=40 sec.

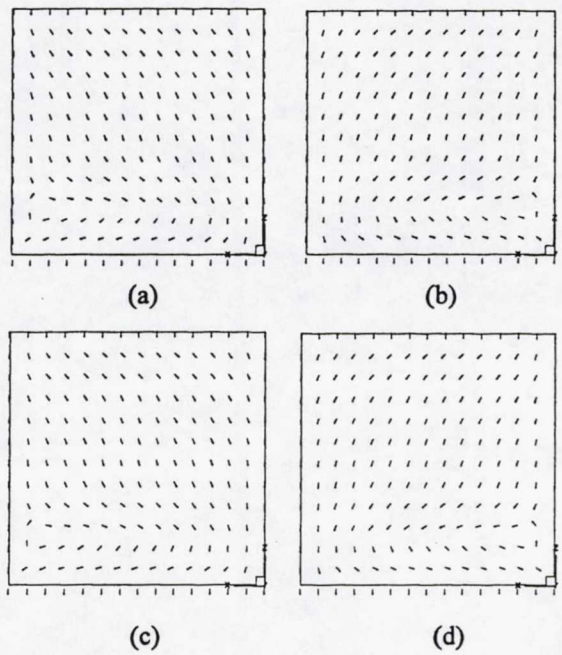

Fig. 6 Magnetically damped velocity field in the x-z plane corresponding to Fig. 4 but with an applied magnetic field in the x-direction B=0.22 Tesla.

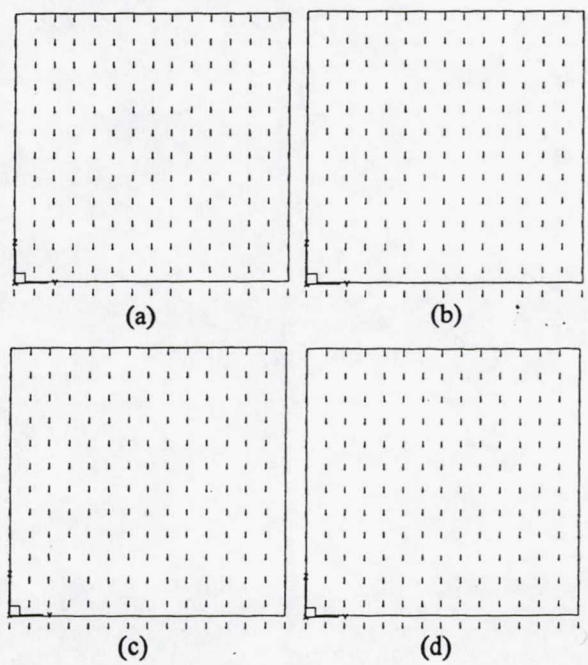

Fig. 7 Magnetically damped velocity field in the y-z plane corresponding to Fig. 5 but with an applied magnetic field in the x-direction B=0.22 Tesla.

Figures 4 and 5 illustrate the fluid flow pattern in the x-z and y-z planes cut at different times after the time varying g-jitter effect comes into play. The three dimensional nature of the flow field is clear. In the y-z plane (or y=0 plane), there exists a g-jitter component oscillating time harmonically along the x-axis. The oscillating gravity force produces an oscillating recirculating convective flow field in the plane. This picture is very similar to the 2-D case where a similar g-jitter gravity force is acting[20].
In the y-z (or x=0) plane where no g-jitter gravity force is present, the situation is quite different in that no recirculating flows are induced and there exists almost no noticeable change in flow pattern (see Figure 5). Detailed analyses showed that the flow pattern in the other planes cut along the z-axis is somewhat between the above two, as expected.

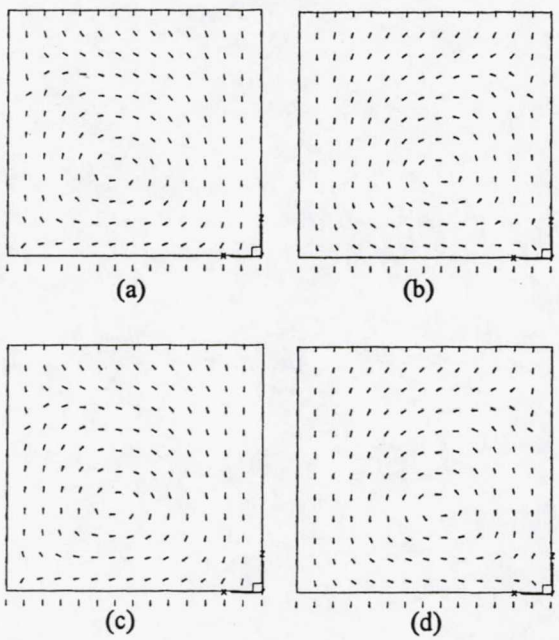

Fig. 8 Magnetically damped velocity field in the x-z plane corresponding to Figure 4 but with an applied magnetic field in the y-direction B=0.22 Tesla.

Let us now turn to the magnetic effects on the g-jitter driven flows. Figures 7 and 8 depict the convective flow field in the x-z and y-z planes with an applied magnetic field oriented in the x-direction and with a field strength of 0.22 Tesla. Comparison of figures 4 and 6 clearly suggests that the applied magnetic has a strong effect on

the g-jitter driven flows. The strong recirculation induced by g-jitter is substantially reduced and recirculation is suppressed in the region right above the lower side. In the y-z plane, the velocity field becomes virtually a plug field and the disturbance resulting from g-jitter is almost completely damped out, as appear in figures 5 and 7.

From the theory of magnetic damping, the opposing Lorentz force depends on not only on the field strength but also its orientation. Figure 8 plots the velocity field in the x-z plane with a magnetic field oriented in the y-direction but with the same field strength as in Figure 6. By comparing figures 4, 6 and 8, it is clear that the magnetic field in the y-direction seems to produce a relatively smaller damping effect on the fluid flow in the x-z plane, as evidenced by the relatively strong convective recirculation persisting in the entire cavity. There is a reduction by the applied magnetic field but the extent to which reduction occurs is apparent less than by applying the magnetic field in the x-direction. However, in the y-z plane, the fluid velocity field is basically reduced by the magnetic field to a plug flow field, very similar to that shown in Figure 7.

(figure will be insert here)

Fig.9 Magnetically damped velocity field in the x-z plane corresponding to Figure 4 but with an applied magnetic field in the z-direction B=0.22 Tesla.

By orienting the magnetic field in the z-direction while maintaining the same field strength, the fluid flow field in the x-z plane becomes different as shown in Figure 9. In this case, the recirculating flow induced by g-jitter is almost completely damped out and flow becomes approximately a plug flow. Analyses further indicated that in the y-z plane, the flow field is reduced also and a velocity field very similar to that in Figure 5 is obtained. These results seem to suggest that for this particular configuration, the maximum damping effect is achieved when the magnetic field is oriented in the z-direction.

5. Concluding Remarks

This paper has presented a 3-D numerical model for the study of transient g-jitter induced convective flows and magnetic damping effects in a simplified Bridgman-Stockbarger system for the melt growth of Ga-doped germanium single crystals. The model was developed based on the Galerkin finite element solution of tranient Navier-Stokes equations, thermal balance and solutal transport equations, and the simplified Maxwell equations. The results show that g-jitter induced flows are complex and three dimensional, evolve in time and oscillate in approximately the same frequency of the acting g-jitter force. For the system studied, a moderate magnetic field can achieve adequate flow reduction. The orientations of the magnetic field also play an important role in the reduction of the convective flows induced by g-jitter.

6. Acknowledgement

Financial support of this work by NASA Microgravity Division (Grant #: NAG8-1477) is gratefully acknowledged.

References

1) S. Lehoczky, F. R. Szofran and D. C. Gillies: *Six Months Sciences Report*, NASA MSC, 1994.

2) H. C. de Groh and E. S. Nelson: ASME Winter Annual Meeting, Chicago, IL, HTD-Vol. **290** (1994) 23

3) J. I. D. Alexander: *Microgravity Sci. Tech.*, **3** (1990) 52.

4) H. Chen, M. Z. Saghir, D. H. H. Quon and S. Chehab: *J. Crystal Growth*, **142** (1994) 362.

5) B. N. Antar and V. S. Nuotio-Antar: *Fundamentals of low gravity fluid dynamics and heat transfer*. CRC Press, Boca Raton, FL, 1993.

6) J. I. D. Alexander: *Microgravity Sci. Tech.*, **7** (1994) 131.

7) J. I. D. Alexander, J. Quazzani and F. Rosenberger: *J. Crystal Growth*, **97** (1989) 285.

8) J. I. D. Alexander, S. Amiroudine, J. Quazzani and F. Rosenberger: *J. Crystal Growth*, **113** (1991) 21.

9) J. Casademunt, W. Zhang, J. Venals and R. F. Sekerka: *AIAA Journal*, **31**(11) (1993) 2027.

10) D. Jacqmin, *J. Fluid Mech.*, **219** (1990) 449.

11) R. J. Naumann: *J. Crystal Growth*, **142** (1994) 253.

12) S. Schneider and J. Straub: *J. Crystal Growth*, **97** (1989) 235.

13) A. A. Wheeler, G. B. McFadden, B. T. Murray and S. R. Coriell: *J. Phys. Fluids* A, **3** (1991) 2847.

14) W. Zhang, J. Casademunt and J. Venals: *J. Phys. Fluids* A, **5** (1993) 3147.

15) W. E. Langlois: *Comput. Methods. Appl. Mech. Eng.*, **25** (1981) 315.

16) W. E. Langlois, K-J Lee: *J. Crystal Growth*, 62 (1993) 481.

17) B. Q. Li: *Int. J. Heat & Mass Trans.*, Vo. 39, No. 14, pp. 2853-2860, 1996.

18) B. Q. Li: *Int. J. Eng. Sci.*, Vol. 34, No. 12, 1996, pp. 1369-1383.

19) B. Pan and B. Q. Li: *Int. J. Heat & Mass Transfer*, to appear.

20) B. Pan, B. Q. Li and H. C. de Groh: *Experimental Methods for Microgravity Materials Science*, Montreal, Canada, May, 1997.